Two-Dimensional Locally Resonant Phononic Crystals with Binary Structures

Gang Wang,* Xisen Wen, Jihong Wen, Lihui Shao, and Yaozong Liu

Institute of Mechatronical Engineering, National University of Defense Technology, Changsha 410073, China and the PBG Research Center, National University of Defense Technology, Changsha 410073, China

(Received 17 June 2004; published 5 October 2004)

The lumped-mass method is applied to study the propagation of elastic waves in two-dimensional binary periodic systems, i.e., periodic soft rubber/epoxy and vacuum/epoxy composites, for which the conventional methods fail or converge very slowly. A comprehensive study is performed for the two-dimensional binary locally resonant phononic crystals, which are composed of periodic soft rubber cylinders immersed in epoxy host. Numerical simulations predict that subfrequency gaps also appear because of the high contrast of mass density and elastic constant of the soft rubber. The locally resonant mechanism in forming the subfrequency gaps is thoroughly analyzed by studying the two-dimensional model and its quasi-one-dimensional mechanical analog. The rule used to judge whether a resonant mode in the phononic crystals can result in a corresponding subfrequency gap or not is found.

DOI: 10.1103/PhysRevLett.93.154302 PACS numbers: 43.40.+s, 46.40.Cd, 63.20.–e

The propagation of elastic or acoustic wave in periodic heterogeneous materials has received much renewed attention in recent years [1–10]. Because of the periodicity of such structures, there exist frequency ranges in which waves are forbidden, giving rise to phononic band gaps which are analogous to photonic band gaps [11–13] for electromagnetic waves. These new materials can be of real interest because of the rich physics of acoustic and elastic systems, where the wave can have mixed longitudinal and transverse modes, and where a large contrast between the elastic parameters is allowed. For example, locally resonant (LR) phononic crystals (PCs) consisting of very soft rubber [1,4,9] (with an elastic constant of five orders lower than common solids) and other components are most likely to obtain the low-frequency gaps with a structure of small dimensions, which can lead to promising applications such as low-frequency vibration or noise insulations.

The lumped-mass (LM) method [7] is proposed recently by us as a new way to compute the band structure of two-dimensional (2D) PCs. The idea of the LM method is the discretization of the continuous system. Thus, the density of the medium is concentrated on discrete points as particles and the elastic constants are treated as linear elasticity between the adjacent particles. By employing a finite number of particles in one period, the band structure can be calculated numerically with our discrete model. Compared with other techniques, the LM method converges faster and its convergence is independent of the sharp variation of elastic constants on the interfaces inside the PCs [7]. We improved the method [8] by replacing the rectangular cells with arbitrary triangular ones in order to describe the topologic structure in a lattice of PCs more precisely.

Up to now, the LR PCs are all ternary systems, which consist of a cubic array of coated spheres [1,3] immersed in epoxy or of a lattice of coated cylinders [4] in epoxy (the coatings are thin films of soft rubber). They predicted the existence of gaps in a frequency range of 2 orders of magnitude lower than the one resulting from the Bragg scattering mechanism, and explained the origin of this phenomenon as due to the localized resonances associated with scattering units. Two-dimensional PCs composed of lattices of polyethylene cylinders in Al were previously researched [6], where no complete gap was observed and where optical-like flat branches were found in the band structure. The first flat branch locates at 1.9 in the reduced frequency unit, corresponding to a lattice vibration mode localized in the softer material (polyethylene).

Here, in order to discover the rule used for judging whether a LR mode can result in a corresponding subfrequency gap or not, we analyze the binary counterparts of the LR PCs which consist of a lattice of soft rubber cylinders in epoxy.

First, we consider two of the same square lattices of soft rubber (the same as Refs. [1,4,9]) and vacuum cylinders in epoxy with a filling fraction $f_h = \pi(r/a)^2 = 0.503$, where r is the radius of the cylinder and $a = 20$ mm is the lattice constant. The elastic constants employed in the calculations are $\rho_{\mathrm{epo}} = 1180\ \mathrm{kg\,m^{-3}}$, $\lambda_{\mathrm{epo}} = 4.43 \times 10^9$ Pa, $\mu_{\mathrm{epo}} = 1.59 \times 10^9$ Pa, $\rho_{\mathrm{rub}} = 1300\ \mathrm{kg\,m^{-3}}$, $\lambda_{\mathrm{rub}} = 6 \times 10^5$ Pa, and $\mu_{\mathrm{rub}} = 4 \times 10^4$ Pa. Figure 1 illustrates the dispersion relations in the rubber/epoxy PCs. The out-of-plane modes [dashed lines in Fig. 1(a)] as well as the in-plane ones [solid lines in Fig. 1(b)] are computed with the LM method by employing 327 particles. The insets represent the corresponding zooms. The frequencies are given in reduced units $\omega a/2\pi c_{t,\mathrm{epo}}$, where $c_{t,\mathrm{epo}}$ is the transverse wave velocity in epoxy. For the vacuum-epoxy PCs, we make the similar calculations and plot the dispersion relations in Fig. 2.

A remarkable feature in Fig. 1 is the flat branches crossing the whole Brillouin zone. These flat branches are real and converged, corresponding to the resonant modes illustrated in Figs. 3 and 4. Some of them split

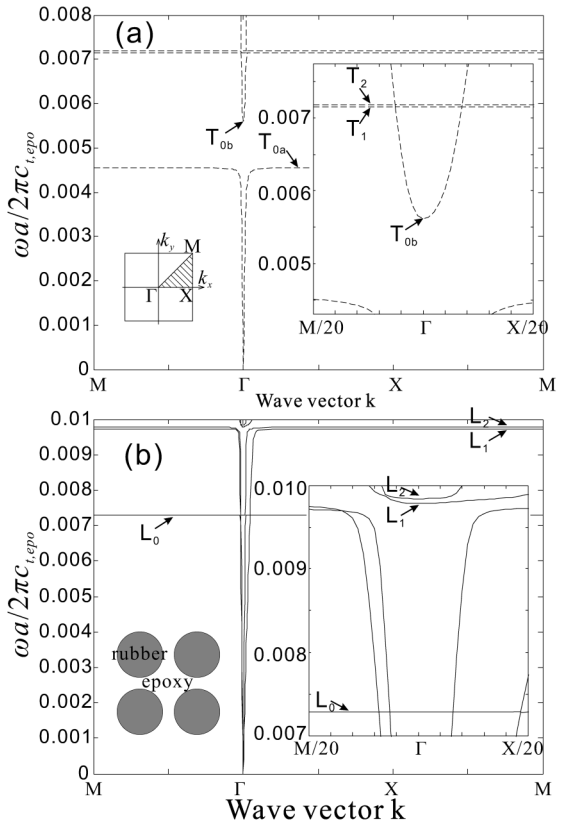

FIG. 1. Dispersion relations of (a) out-of-plane modes and (b) in-plane modes in binary PCs composed of the square lattice of soft rubber cylinders in epoxy. The insets show the corresponding zooms.

the original dispersion curves (illustrated in Fig. 2) of the vacuum-epoxy PCs, while the others just thrill through them.

In detail, from Figs. 1(a) and 3, we can observe a subfrequency gap in the frequency range from 0.0046 to 0.0058 (in reduced units), which is 2 orders of magnitude lower than the one resulting from Bragg scattering, as observed in ternary cases [1,4]. This subfrequency gap results from the first resonant mode plotted in Figs. 3(a) and 3(b). At point T_{0a} [Fig. 3(a)], the amplitude of the vibrations is well concentrated in the region of rubber cylinders, and it is very small in the hosting media. At point T_{0b} [Fig. 3(b)], the lattice vibrations are almost the same except that the vibrations in the hosting media are notable and in the reverse phase of that in the cylinders. For both cases, rubber cylinders vibrate as mass-spring oscillators. The time harmonic forces from oscillators to the hosting structure split the original dispersion curves, and a narrow gap is generated. As for the second and third resonant modes illustrated in Figs. 3(c) and 3(d), which look like the field map of a dipole, the forces from the rubber oscillator to the hosting structure are counteracted. Their corresponding flat branches in the band structure thrill through the original dispersion curves and no gap is generated.

For the in-plane modes shown in Fig. 1(b), the first resonant mode illustrated in Fig. 4(a) looks like a clockwork torsion spring. Because of the aforesaid reason, i.e., the composition of the forces to the hosting structure contributed by the oscillator is zero, its corresponding flat branches in band structure just thrill through the original dispersion curves and no gap is generated. As for the second and third resonant modes illustrated in Figs. 4(b) and 4(c) where the compositions of forces are not zero, the dispersion curves are cut off at their corresponding eigenfrequencies (0.009 88 and 0.009 96 in reduced units) in Fig. 1(b).

In order to support the resonant origin of the subfrequency gaps, we plot in Fig. 5 the dependency on f_h of the band edges determining the lowest gap of the out-of-plane modes. In Figs. 5(a) and 5(b) the lattice constant a is a constant, while in Fig. 5(c) the radius of the soft rubber cylinder r keeps constant as 8 mm. The behavior of

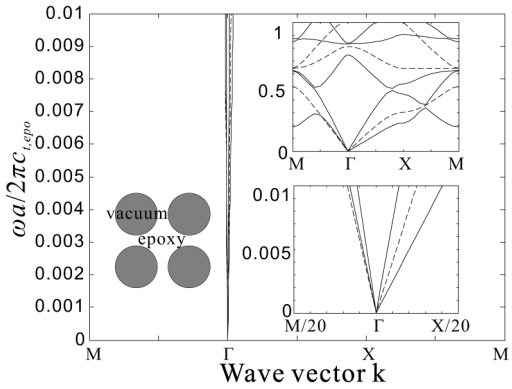

FIG. 2. Dispersion relations of in-plane (solid lines) and out-of-plane mode (dashed lines) in the PCs composed of the square lattice of vacuum cylinders in epoxy. The insets show the zooms.

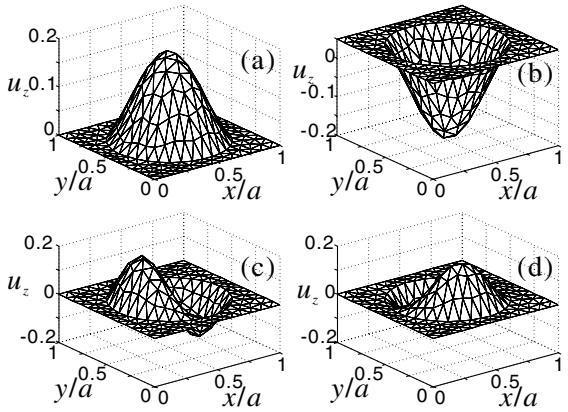

FIG. 3. Lattice displacement u_z (the component parallel to the cylindrical axis) in rubber/epoxy PCs, the same as for Fig. 1. The selected modes are corresponding to points (a) T_{0a}, (b) T_{0b}, (c) T_1, and (d) T_2 in Fig. 1(a), respectively.

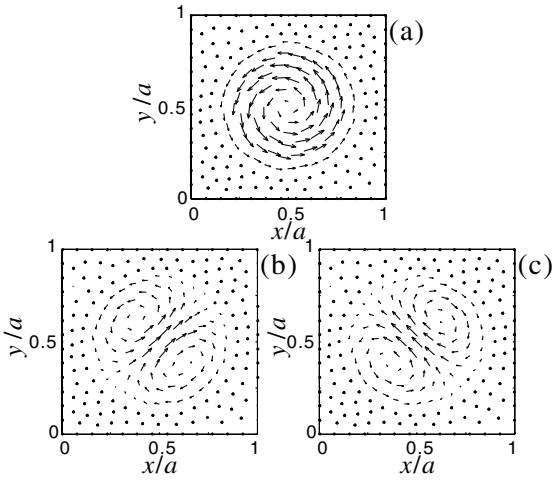

FIG. 4. Lattice displacement vector u_{xy} (the mixed vector vertical to the cylindrical axis) in rubber/epoxy PC, the same as for Fig. 1. The direction and length of the arrows represents the direction and amplitude of the displacement vectors, respectively. The selected modes are corresponding to points (a) L_0, (b) L_1, and (c) L_2 in Fig. 1(b), respectively.

the band edges is completely different from that characterizing a Bragg gap (see, for example, Fig. 2 in Ref. [4] or Fig. 3 in Ref. [9]). The upper panel shows that the reduced frequencies of both edges reduce with f_h. This is a signature of their resonant origin. The pinning of the edges are a consequence of their resonant characters of their associated modes. Particularly, the bottom edge corresponds to the localized vibration mode inside the rubber, where the eigenfrequency is determined by the oscillator consisting of rubber only. The upper edge corresponds to the vibration mode where the epoxy is also involved. So the eigenfrequency of the upper edge is

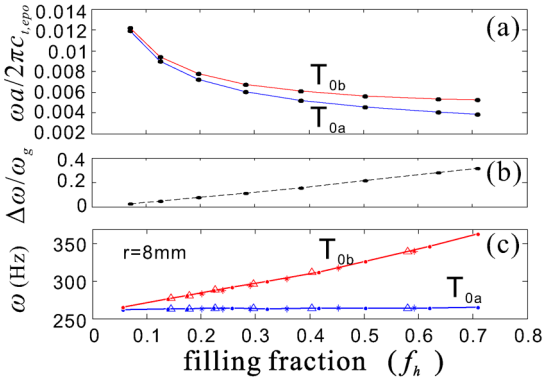

FIG. 5 (color online). (a) The band edges determining the first gap of out-of-plane modes in the 2D binary LR PCs for several filling fractions (f_h). (b) Behavior of the corresponding normalized gap width. (c) Edges of the first gap in 2D binary LR PCs with honeycomb (stars), triangular (triangles), and square (filled circles) lattices for several f_h. In (c), the frequencies are given in Hz, and the radius of the soft rubber cylinders r is kept constant while only the lattice constant a changes.

slightly higher than the previous one. In Fig. 5(c) where the radius of the rubber cylinders is a constant, the real frequency of the lower edge keeps constant no matter how other parameters such as lattice types or lattice constants change. As a result, band gaps in such a system will also appear even in the absence of periodicity. This is a signature of its localized nature.

In order to understand the physical insight of the complicated system more clearly, we introduce a simple quasi-one-dimensional analog model. As shown in Fig. 6(a), the model consists of a linear beam with oscillators periodically attached to it. The Yang's module, cross section area, and length density of the beam are $E = 8 \times 10^9$ Pa, $S = 4 \times 10^{-4}$ m^2, and $\rho_l = 2.8$ kg/m, respectively. The lattice parameters are $a_A = 19$ mm and $a_B = 1$ mm. Each oscillator consists of two equal masses ($m_1 = m_2 = 16$ g) and three springs ($k_1 = k_2 = 38\,000$ N/m and $k_m = 24\,700$ N/m). The parameters are chosen in order to fit the 2D binary LR PCs as for Fig. 1(a).

The mechanical system can be solved analytically by the transfer matrix method [14]. The corresponding band structure is illustrated in Fig. 6(b).

In Figs. 6(b) and 7, we can observe similar characters shown in Figs. 1(a) and 3. A subfrequency gap exists in the same frequency range as appears in Fig. 1(a). This subfrequency gap results from the first resonant mode plotted in Figs. 7(a) and 7(b). At point B_{0a}, the vibration of the system is well concentrated on the oscillators where

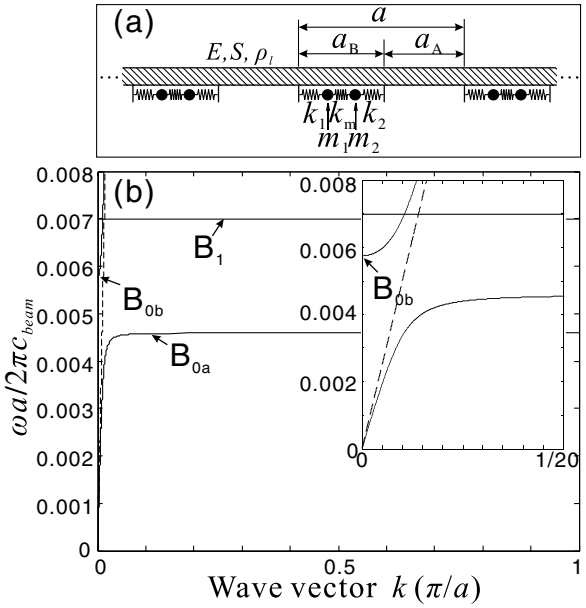

FIG. 6. (a) The quasi-one-dimensional analog model which is used to understand the physical insight of the 2D LR PCs. (b) Band structure of the analog model (solid lines) or just a single beam (dashed lines). The frequencies are given in reduced units $\omega a/2\pi c_{\text{beam}}$, where c_{beam} is the longitudinal wave velocity in the beam.

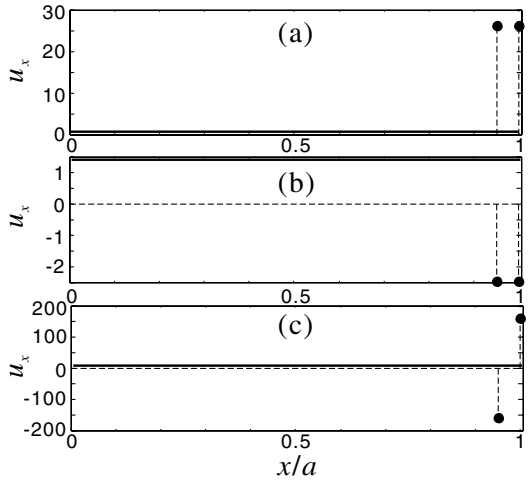

FIG. 7. The displacements u_x of the beam (solid line) and of the two masses (filled circles). The selected modes are corresponding to points (a) B_{0a}, (b) B_{0b}, and (c) B_1 in Fig. 6(b), respectively.

the two masses vibrate with the same phase and amplitude. So the eigenfrequency of the lower edge of the gap can be calculated with

$$\frac{a}{2\pi c_{\text{beam}}}\sqrt{\frac{k_1+k_2}{m_1+m_2}} = 0.0046. \quad (1)$$

At point B_{0b} [Fig. 7(b)], the mode is almost the same except that the vibration of the beam is not zero and in reversed phase to that of the masses. Its eigenfrequency that determines the upper edge of the gap can be calculated with

$$\frac{a}{2\pi c_{\text{beam}}}\sqrt{\frac{k_1+k_2}{m_1+m_2}\left(1+\frac{m_1+m_2}{\rho_l a}\right)} = 0.0058. \quad (2)$$

For both points B_{0a} and B_{0b} [Fig. 7(b)], the time harmonic forces from the oscillators to the beam split the original dispersion curves [of the beam only, illustrated as dashed lines in Fig. 6(b)]. A subfrequency gap is then generated. As for the second resonant mode illustrated in Fig. 7(c) where the two masses vibrate with reversed phases, the forces from the oscillator to the beam are counteracted. Their corresponding flat branches in the band structure thrill through the original dispersion curves and no gap is generated. Its eigenfrequency can also be calculated with

$$\frac{a}{2\pi c_{\text{beam}}}\sqrt{\frac{k_1+2k_m}{m_1}} = 0.007. \quad (3)$$

In conclusion, we have studied the propagation of elastic waves in two-dimensional binary phononic crystals consisting of lattices of soft rubber cylinders in epoxy, i.e., the binary locally resonant materials. Numerical simulations predict that the subfrequency gap also appears because of the high contrast of mass density and elastic constants of the soft rubber. The locally resonant mechanism is proved adequately and analyzed deeply. A simple quasi-one-dimensional mechanical analog model is introduced in order to understand the physical insight of the locally resonant mechanism more clearly. We discover for the first time the rule used to judge whether a resonant mode in the phononic crystals can result in a corresponding subfrequency gap or not.

Support from the State Key Development Program for Basic Research (Grant No. 51307) of China is gratefully acknowledged.

*Electronic address: wang-g@vip.sina.com

[1] Z. Liu, X. Zhang, Y. Mao, Y. Y. Zhu, Z. Yang, C. T. Chan, and P. Sheng, Science **289**, 1734 (2000).
[2] R. Martínez-Sala, J. Sancho, J. V. Sánchez, V. GómezJ. Llinares, and F. Meseguer, Nature (London) **378**, 241 (1995).
[3] Z. Liu, C. T. Chan, and P. Sheng, Phys. Rev. B **65**, 165116 (2002).
[4] C. Goffaux and J. Sánchez-Dehesa, Phys. Rev. B **67**, 144301 (2003).
[5] C. Goffaux, J. Sánchez-Dehesa, A. L. Yeyati, P. Lambin, A. Khelif, J. O. Vasseur, and B. Djafari-Rouhani, Phys. Rev. Lett. **88**, 225502 (2002).
[6] Y. Tanaka, Y. Tomoyasu, and S. I. Tamura, Phys. Rev. B **62**, 7387 (2000).
[7] G. Wang, J. Wen, Y. Liu, and X. Wen, Phys. Rev. B **69**, 184302 (2004).
[8] G. Wang, J. Wen, D. Yu, Y. Liu, and X. Wen (to be published).
[9] G. Wang, D. Yu, J. Wen, Y. Liu, and X. Wen, Phys. Lett. A **327**, 512 (2004).
[10] G. Wang, J. H. Wen, X. Y. Han, and H. G. Zhao, Acta Phys. Sin. **52**, 1943 (2003).
[11] E. Yablonovitch, Phys. Rev. Lett. **58**, 2059 (1987).
[12] S. John, Phys. Rev. Lett. **58**, 2486 (1987).
[13] S. G. Johnson and J. D. Joannopoulos, *Photonic Crystals—The Road from Theory to Practice* (Kluwer Academic, Dordrecht, 2002).
[14] B. Djafari-Rouhani, L. Dobrzynski, O. HardouinDuparc, R. E. Camley, and A. A. Maradudin, Phys. Rev. B **28**, 1711 (1983).